

Supplementary Figures

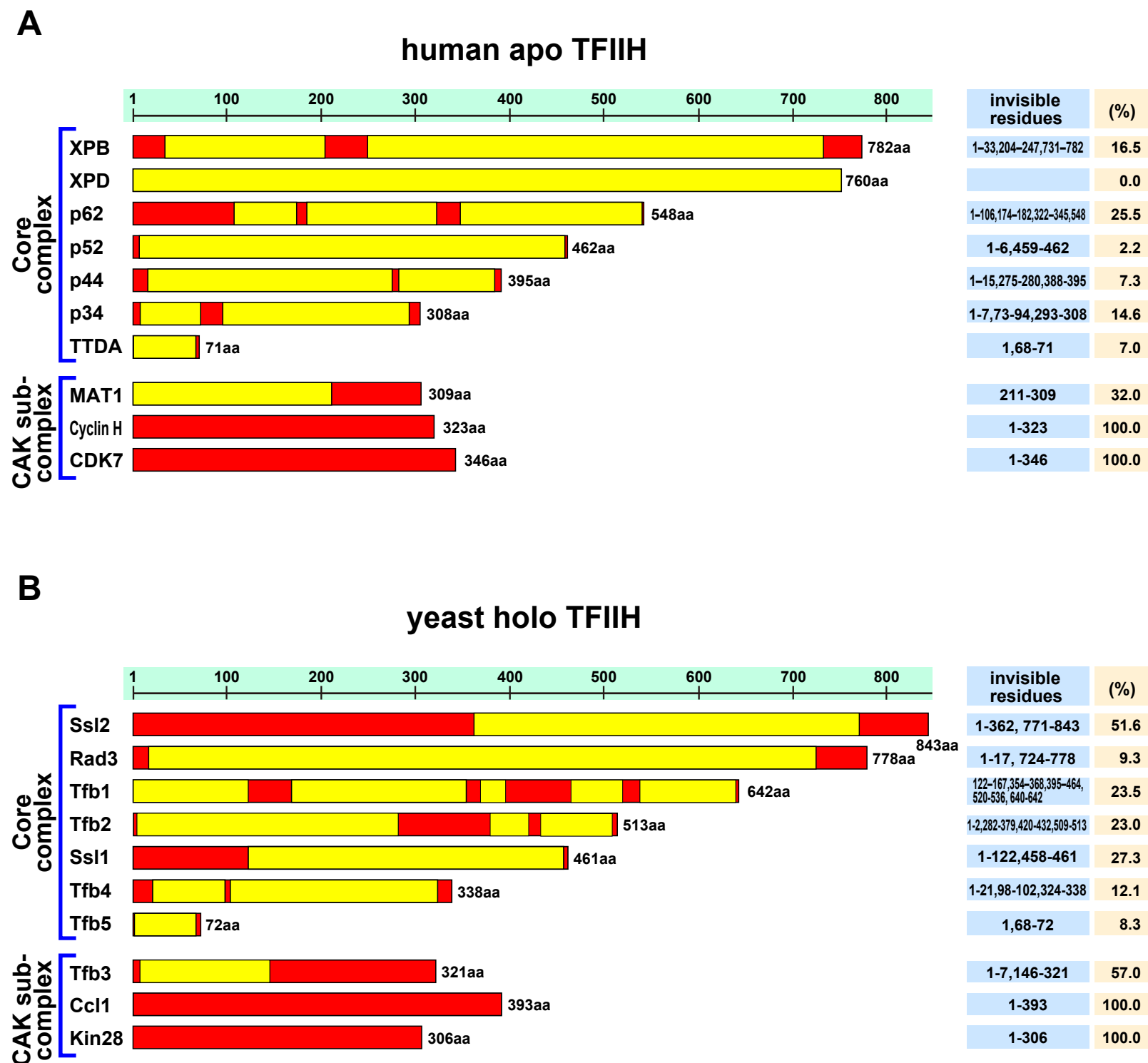
Structural and dynamical insights into the PH domain of p62 in human TFIIH

Masahiko Okuda¹, Toru Ekimoto¹, Jun-ichi Kurita¹, Mitsunori Ikeguchi^{1,2} and Yoshifumi Nishimura^{1,3}

¹ Graduate School of Medical Life Science, Yokohama City University, 1-7-29 Suehiro-cho, Tsurumi-ku, Yokohama 230-0045, Japan

² RIKEN Medical Sciences Innovation Hub Program, 1-7-22 Suehiro-cho, Tsurumi-ku, Yokohama 230-0045, Japan

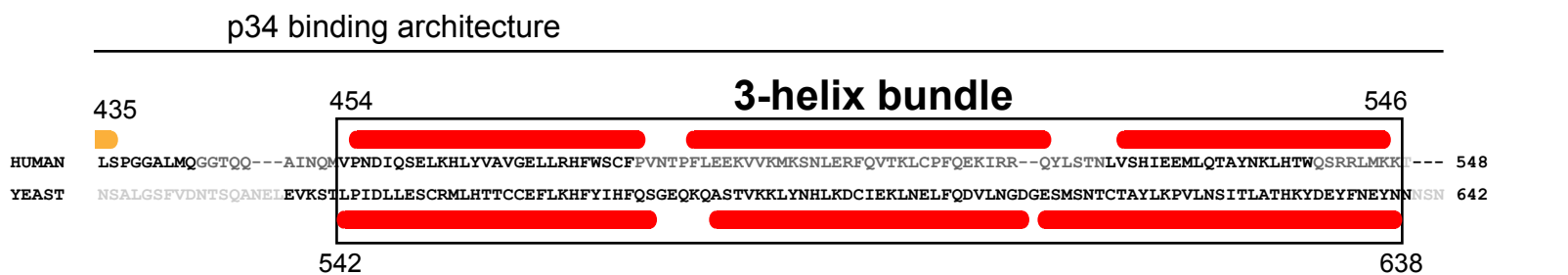
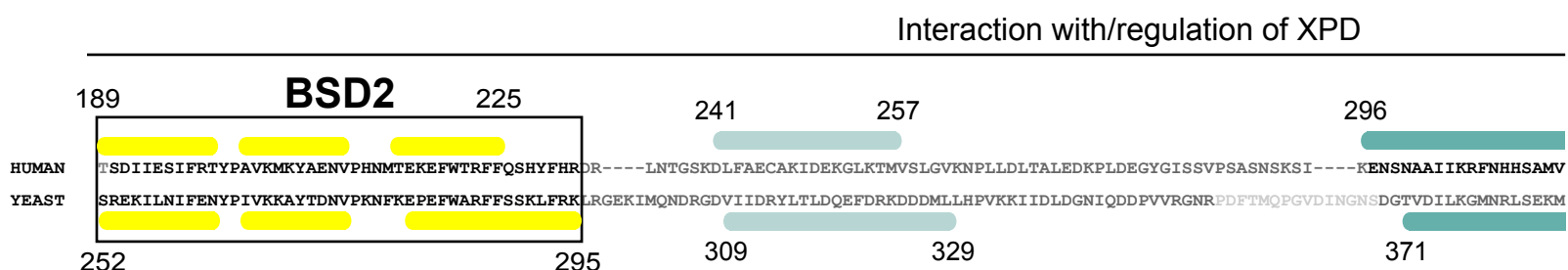
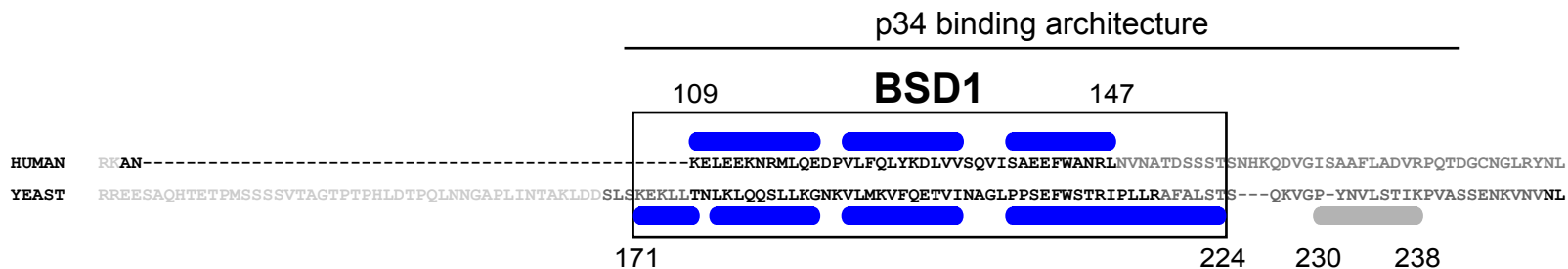
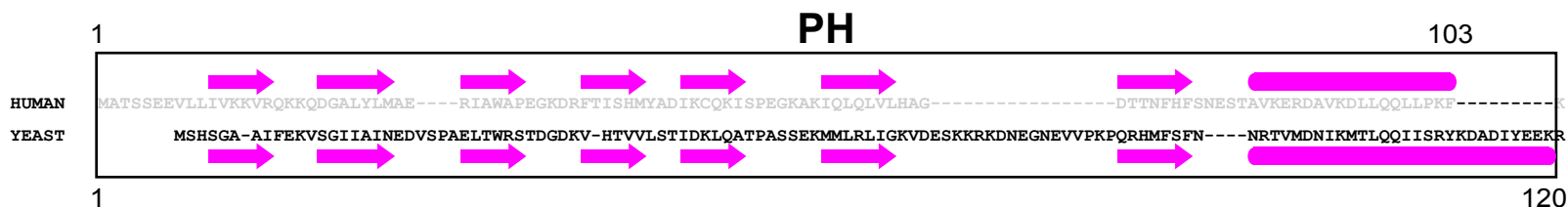
³ Graduate School of Integrated Sciences for Life, Hiroshima University, 1-4-4 Kagamiyama, Higashi-Hiroshima 739-8258, Japan



Supplementary Figure S1. Visible and invisible regions of the Cryo-EM structures of the human apo and yeast holo TFIIH Core complexes.

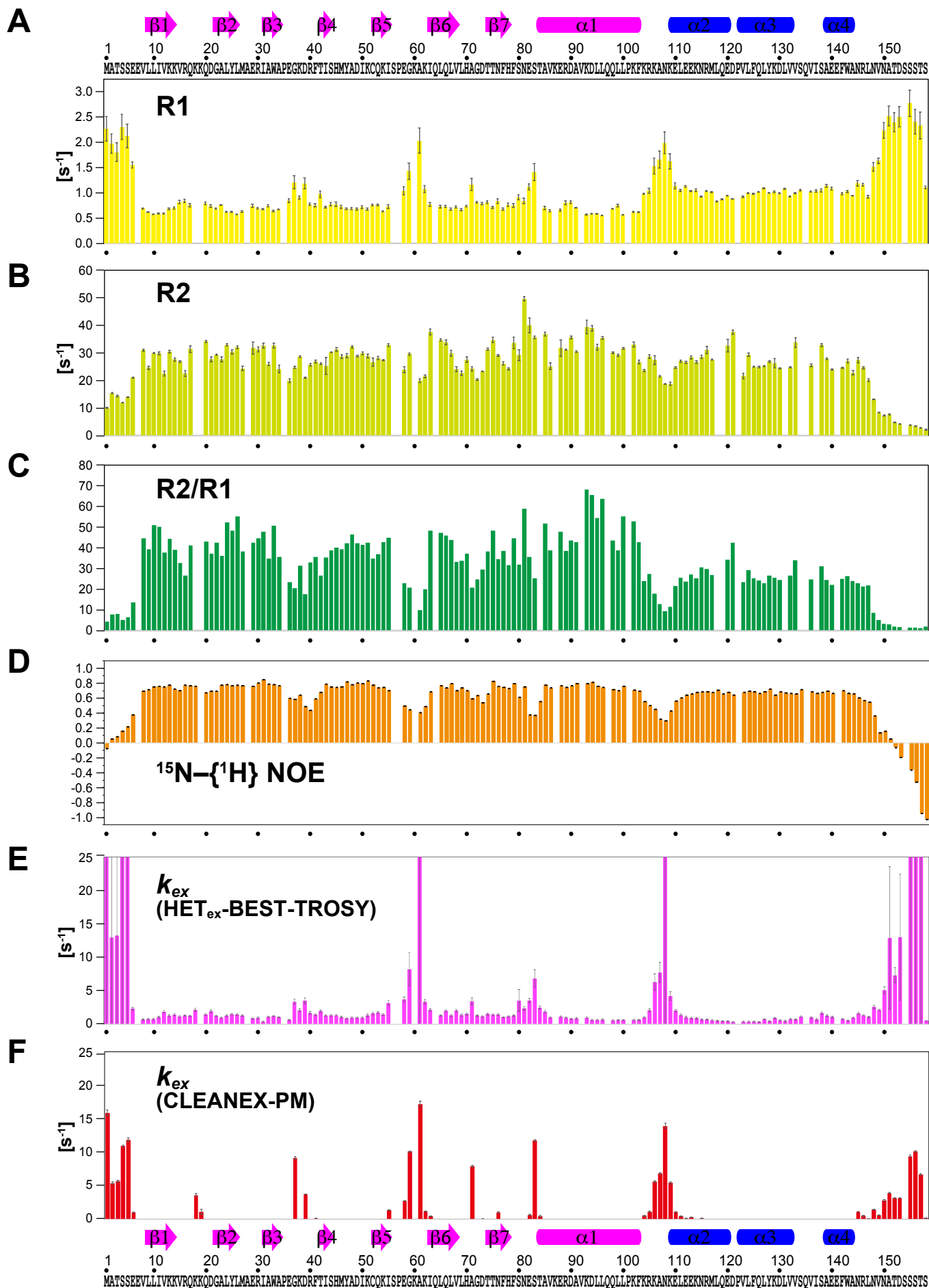
(A and B) The 10 subunits of human (A) and yeast (B) TFIIH. Regions that are visible in the Cryo-EM structures of the human apo TFIIH Core complex (PDB ID: 6NMI) and yeast holo TFIIH Core complex (PDB ID: 5OQJ) are shown in yellow; those that are invisible are shown in red. Invisible residues and their percentage in each subunit are indicated on the right.

Interactions with PIC, activators, NER machinery



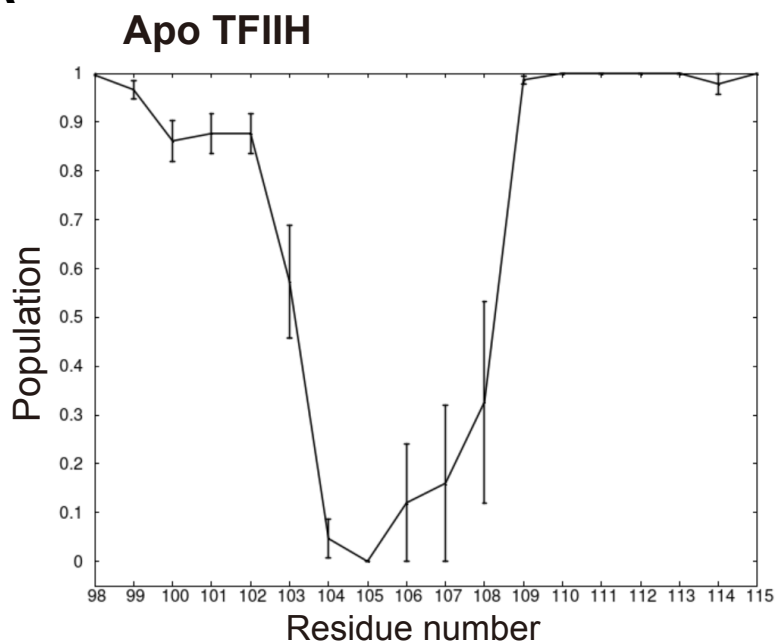
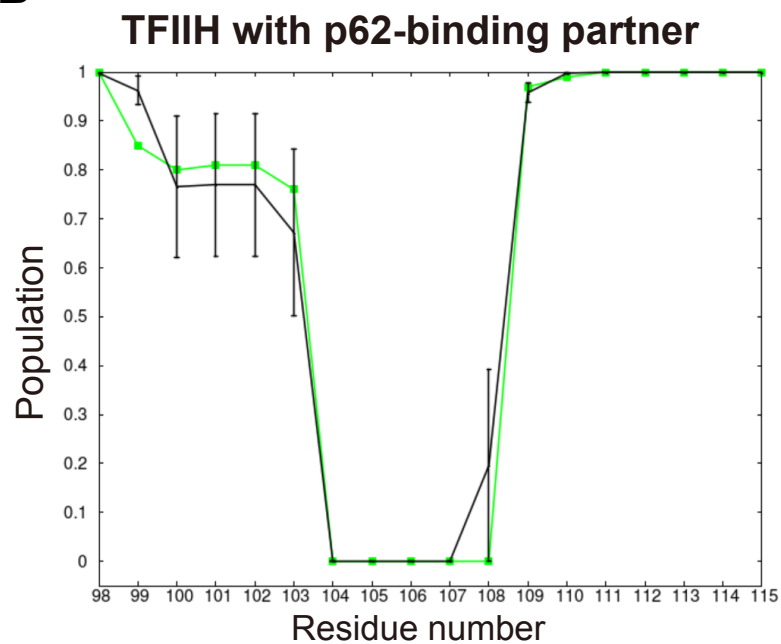
Supplementary Figure S2. Sequence alignment of human p62 and yeast Tfb1.

Light gray indicates amino acids not seen in the Cryo-EM structure. Gray indicates unidentified amino acids. Arrows and bars above and below the sequence indicate β -strands and α -helices, respectively.



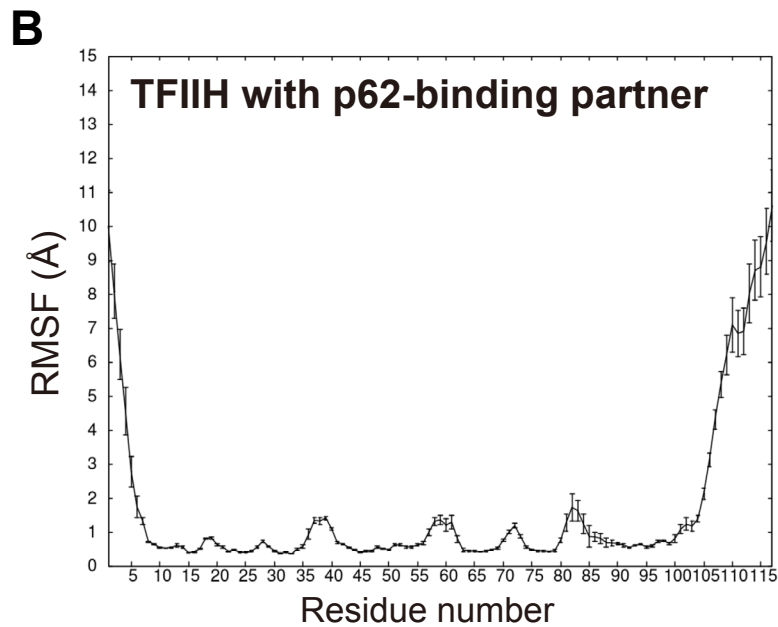
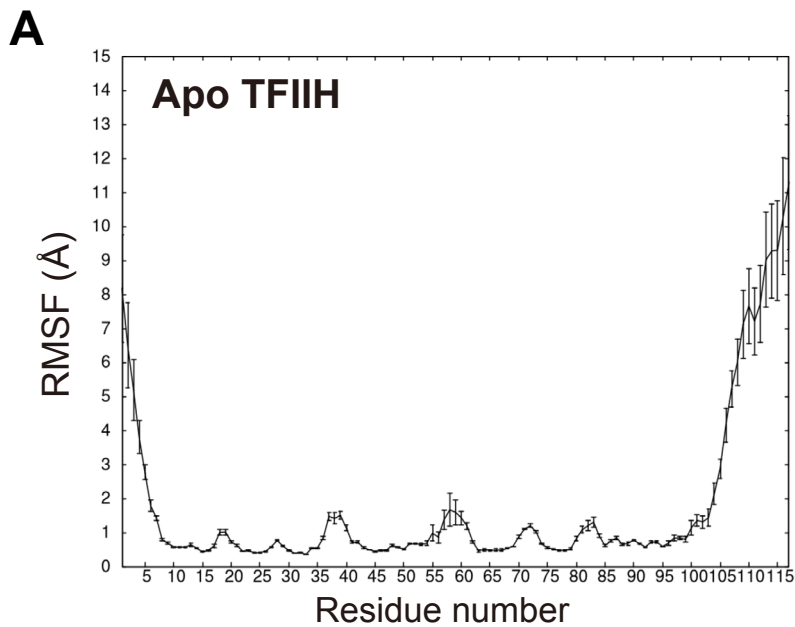
Supplementary Figure S3. Dynamics of the PH and BSD1 domains of human TFIIH p62.

(A) ^{15}N longitudinal relaxation rate (R1). (B) Transverse relaxation rate (R2). (C) Ratio of R2 to R1. (D) ^{15}N - $\{^1\text{H}\}$ nuclear Overhauser effect (NOE). (E and F) Water-amide proton exchange rate (k_{ex}) measured by HETex-BEST-TROSY (E) and CLEANEX-PM (F).

A**B**

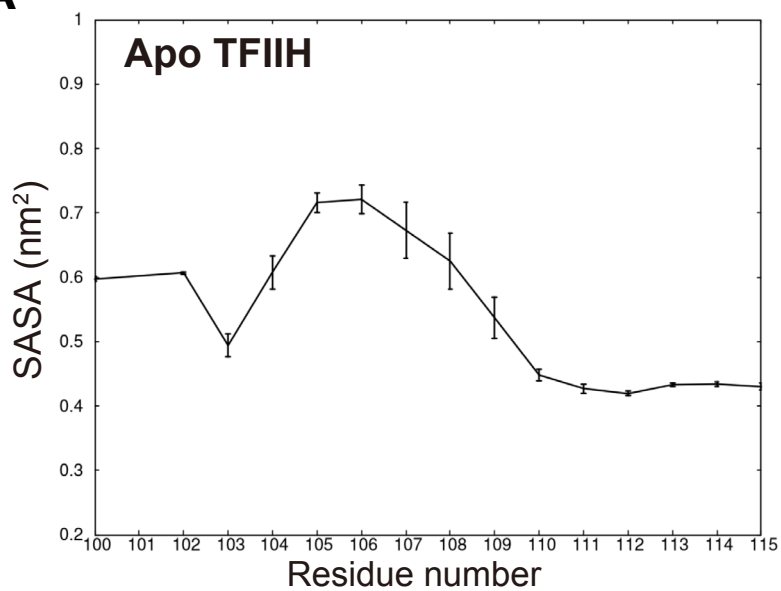
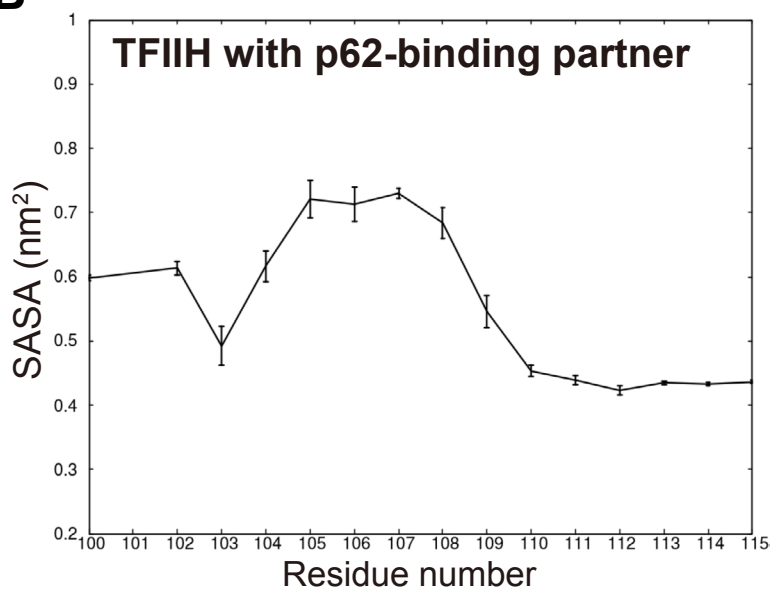
Supplementary Figure S4. Population of helix or 3_{10} helix structures for (A) apo TFIIH and (B) TFIIH with a p62-binding partner.

The population of the helix or 3_{10} helix structures is the average of (A) six or (B) five MD simulations. The green line in (B) indicates the population for the TFIIH in complex with TFII α . The bar represents the standard error.



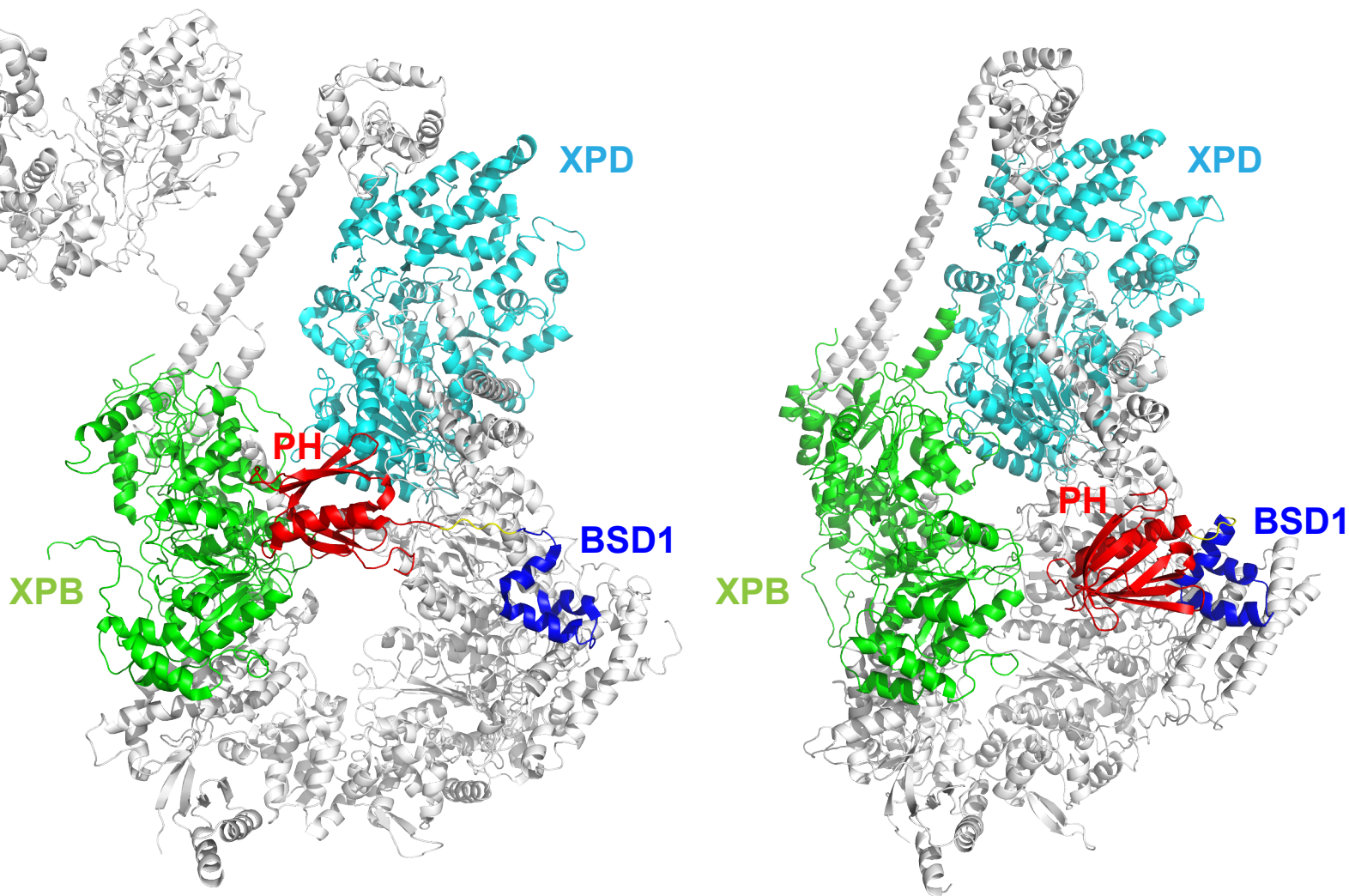
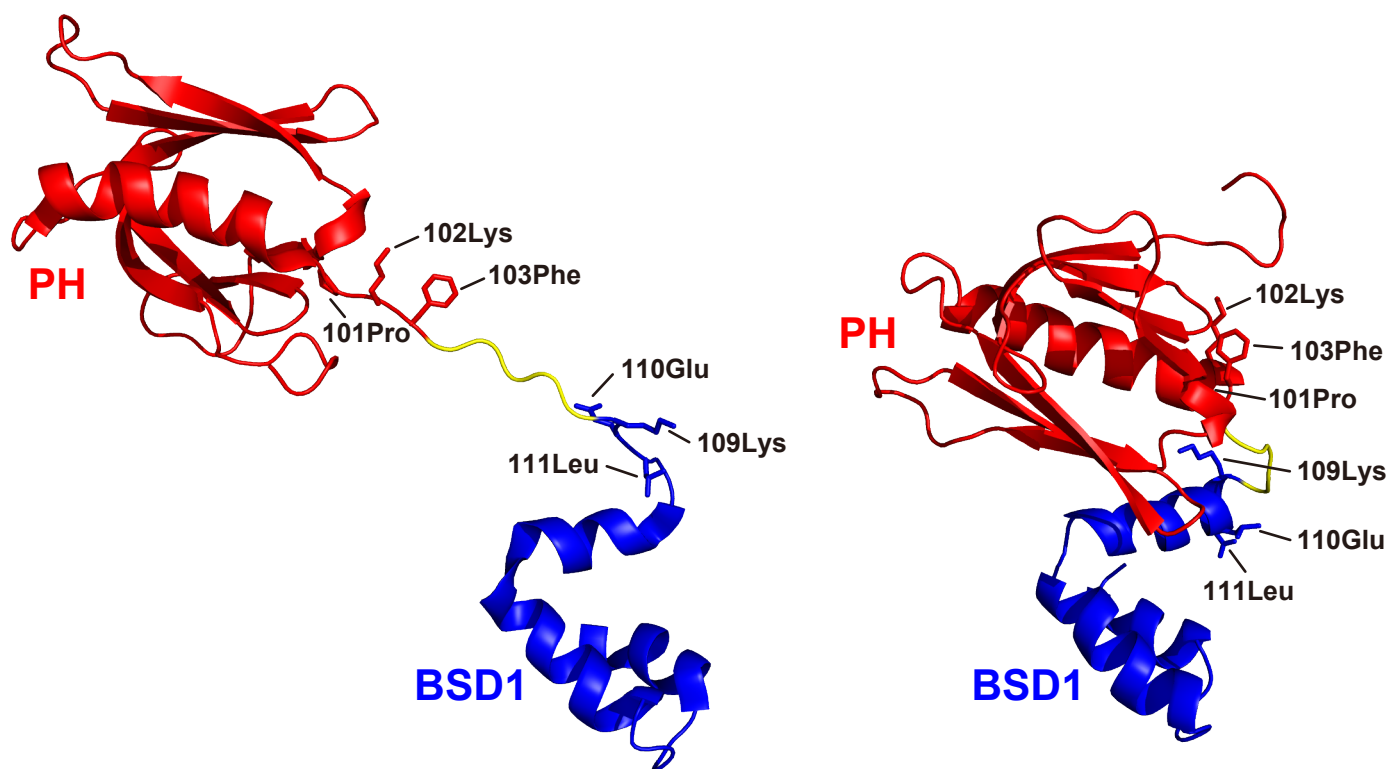
Supplementary Figure S5. Root mean square fluctuation of the PH-D and the linker for (A) apo TFIIH and (B) TFIIH with a p62-binding partner.

The RMSF value of each residue is the average of (A) six or (B) five MD simulations. The bar represents the standard error.

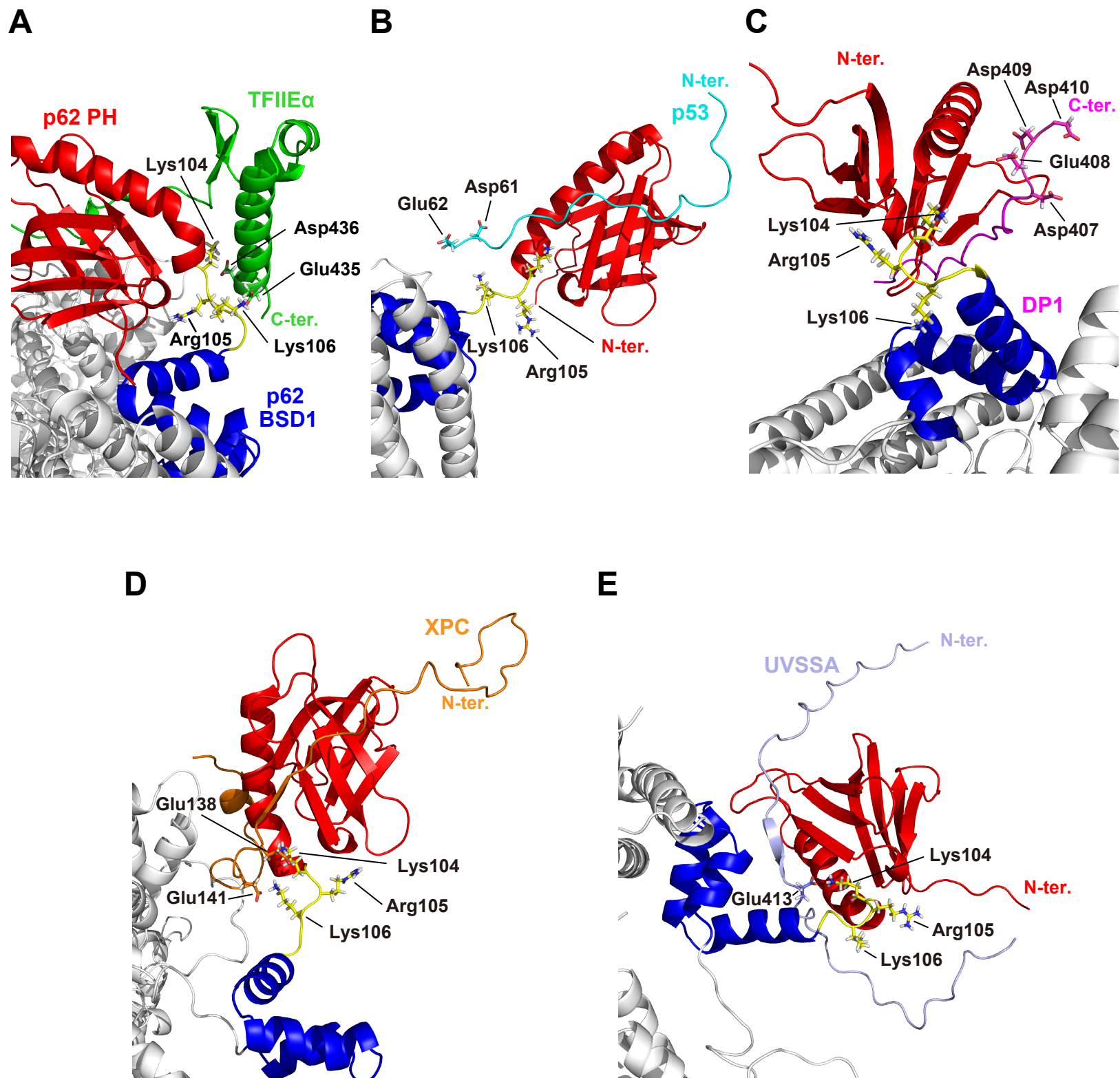
A**B**

Supplementary Figure S6. Solvent-accessible surface area of the amide hydrogens for (A) apo TFIIH and (B) TFIIH with a p62-binding partner.

The SASA value of each residue is the average of (A) six or (B) five MD simulations. The bar represents the standard error.

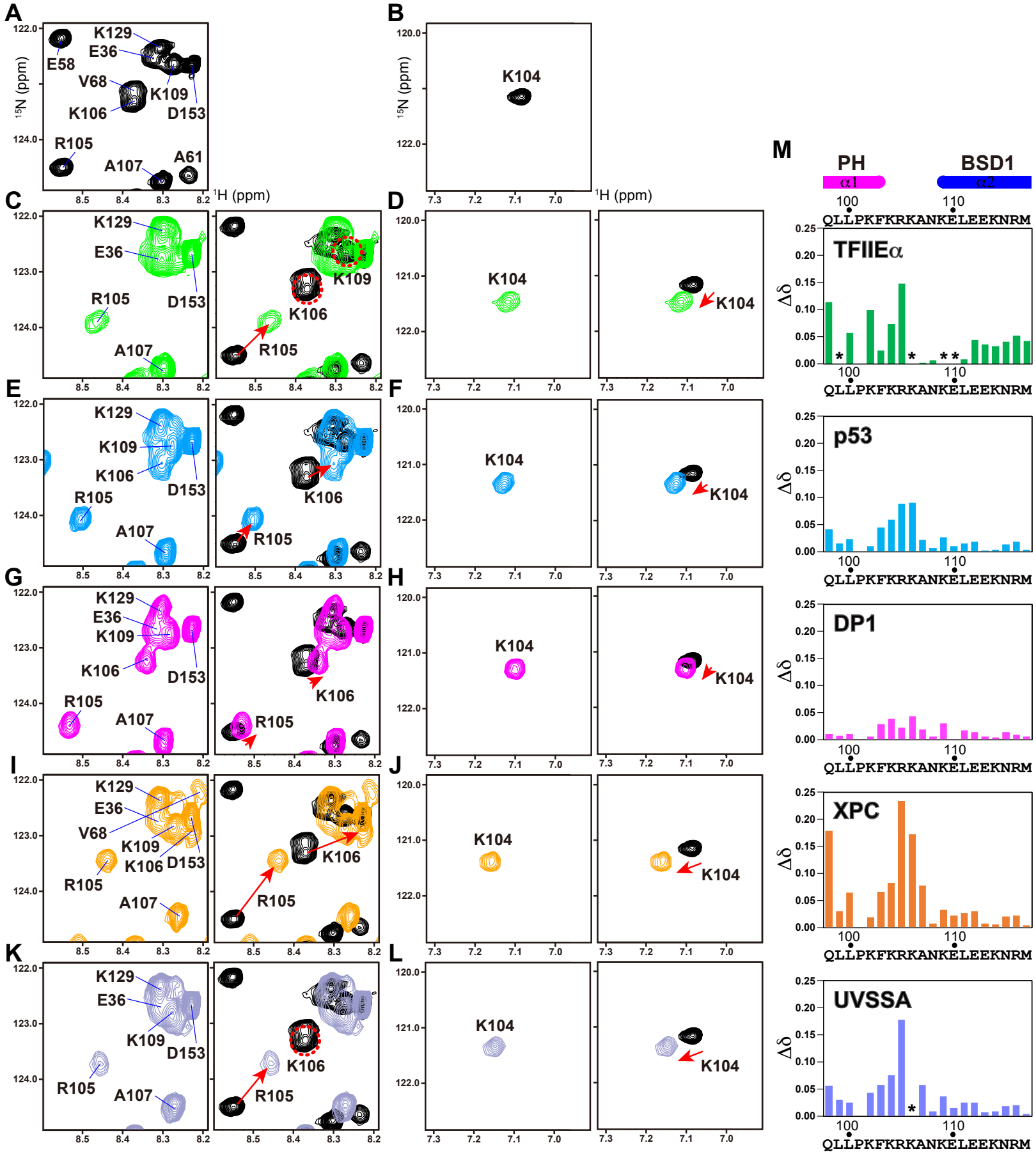
A**B**

Supplementary Figure S7. Structural comparison of the p62 PH-D between the apo and holo TFIIF complexes. (A) Structure of the TFIIF complex. Left, holo TFIIF complex in the PIC (PDB code 6O9L); right, apo TFIIF complex (our structural model). For clarity, only the XPB and XPD subunits, PH-D, linker and BSD1 domain of p62 are colored. (B) Structure of the PH-D and BSD1 domain of p62 in the TFIIF complex. Left, holo TFIIF complex (PDB code 6O9L); right, apo TFIIF complex (our structural model).



Supplementary Figure S8. MD simulation models suggest electrostatic interactions between lysine residues in the linker of p62 and acidic residues around the C-terminus of the binding sites of p62-binding partners.

Complex of TFIIH (gray) with TFIIIE α (green) (A), p53 (cyan) (B), DP1 (magenta) (C), XPC (orange) (D) and UVSSA (light blue) (E). The PH-D, BSD1 domain and linker of p62 are shown in red, blue and yellow, respectively.



Supplementary Figure S9. NMR chemical shift perturbation for the ^{15}N -labeled PH and BSD1 domains of human TFIIH p62 with five p62-binding partners. ^1H , ^{15}N -HSQC spectra of p62 PH and BSD1 domains (black) alone (**A** and **B**) and mixed with TFIIIE α (green) (**C** and **D**), p53 (cyan) (**E** and **F**), DP1 (magenta) (**G** and **H**), XPC (orange) (**I** and **J**) and UVSSA (light blue) (**K** and **L**). An overlay of ^1H , ^{15}N -HSQC spectra before (black) and after the addition of unlabeled p62-binding partner is shown in the righthand panels. Arrows indicate basic residues showing a significant chemical shift change, and dotted circles indicate unassigned signals due to disappearance or overlap with other signals after addition of the unlabeled sample. (**M**) Histogram showing the chemical shift change ($\Delta\delta$) per residue of the inter-domain linker of p62. $\Delta\delta$ was calculated as $\Delta\delta = \{(\Delta\delta^1\text{H})^2 + (\Delta\delta^{15}\text{N}/5)^2\}^{1/2}$. Asterisks indicate residues whose signals were unassigned due to disappearance or overlap with other signals. **10**